ISSN 1063-7834, Physics of the Solid State, 2013, Vol. 55, No. 10, pp. 2057–2064. © Pleiades Publishing, Ltd., 2013.
Original Russian Text © M.N. Dubovik, V.V. Zverev, B.N. Filippov, 2013, published in Fizika Tverdogo Tela, 2013, Vol. 55, No. 10, pp. 1942–1949.

MAGNETISM

Two-Dimensional Micromagnetic Simulation of Domain Structures in Films with Combined Anisotropy

M. N. Dubovik[a, b, *], V. V. Zverev[b], and B. N. Filippov[a]

[a] *Institute of Metal Physics, Ural Branch of the Russian Academy of Sciences, ul. Sofii Kovalevskoi 18, Yekaterinburg, 620990 Russia*

* *e-mail: dubovik@imp.uran.ru*

[b] *Ural Federal University named after the First President of Russia B. N. Yeltsin (Ural State Technical University–UPI), ul. Mira 19, Yekaterinburg, 620002 Russia*

Received March 27, 2013

Abstract—The transformation of the domain structure of micrometer-thick films with variations in the induced uniaxial anisotropy constant with the easy magnetization axis perpendicular to the film surface has been investigated using numerical micromagnetic simulation in the framework of a two-dimensional model of the magnetization distribution. The case where the tetra-axial crystallographic anisotropy exists in the film with uniaxial magnetic anisotropy has been considered. The transformation of the open domain structure into the structure with a magnetic flux closed inside the sample has been investigated in detail, and new types of 109-degree and 90-degree vortex-like domain walls and periodic domain structures have been obtained.

DOI: 10.1134/S1063783413100119

1. INTRODUCTION

Investigation of nonlinear processes responsible for the formation of domain walls and a domain structure in magnets is of great scientific interest, because it has become possible to predict characteristics of new magnetic materials important for practical purposes. In particular, this provides the basis for the development and improvement of technologies for storage and processing of information on magnetic recording media. A theoretical study of these processes is associated, however, with the necessity of solving complex systems of nonlinear differential equations. Analytical solutions for equations of this type can be obtained only in exceptional cases after the introduction of a number of simplifying assumptions (usually, significantly distorting the original statement of the problem). For this reason, problems of the considered type have usually been solved using numerical micromagnetic simulation [1–6].

Among the factors that determine the character of the domain structure and domain walls in a sample of limited size is the type and magnitude of magnetic anisotropy. At present, structures of domain walls with two-dimensional and three-dimensional distributions of the magnetization have been thoroughly studied in magnetically uniaxial films with both perpendicular [7–10] and in-plane [1, 2, 11, 12] anisotropies. In the case of perpendicular anisotropy, researchers have considered films with the quality factor $Q = K/2\pi M_s^2$ (where K is the anisotropy constant and M_s is the saturation magnetization), which can be larger [7–10] and smaller [13] than unity. In all cases, it has been found that there are significant differences between the properties of these domain walls and the properties of a one-dimensional micromagnetic structure, which was calculated for the first time in [14] and has usually been referred to as the Bloch wall. For example, in magnetically uniaxial films with perpendicular anisotropy and a quality factor $Q > 1$, domain walls contain near-surface Néel segments, i.e., regions with the magnetization **M** parallel to the boundary surfaces of the film and perpendicular to the domain wall plane. At the same time, on opposite sides of the film, the magnetization **M** is oriented in opposite directions; hence, these walls have been referred to as the twisted domain walls [15]. Away from the film surface, the magnetization distribution in domain walls of this type approaches the distribution that is characteristic of Bloch walls. Thus, in general, a symmetric magnetization reversal occurs inside the film. In domains separated by these domain walls, the magnetization reaches the surface of the film (open structure), thus forming magnetostatic poles. An externally similar structure of the isolated domain wall was obtained in [13] for a film with perpendicular anisotropy, but with $Q < 1$. However, in the considered case, the domain wall itself is strongly stretched, and the Néel segments on the film surface have a significantly larger volume than those for the quality factor $Q > 1$. Interesting results were obtained for films with a combined type of anisotropy, i.e., with the easy magnetization axis tilted with respect to the surface and the uniaxial in-plane anisotropy. Such an unusual anisotropy appears as a result of oblique deposition of films with a quality fac-

tor $Q < 1$ [16]. In this case, there can arise closed magnetization structures with Néel segments above the domain walls and with near-surface magnetization reversals in domains during the transition from one domain wall to another. It should be noted that, although the distribution of the magnetization **M** in this case resembles the closed Landau–Lifshitz structure [14], they are not equivalent. It has been found that there are three possible strong stripe domain structures that differ by the arrangement of the central domain wall surfaces relative to each other.

In magnetically uniaxial films with in-plane anisotropy, there are asymmetric vortex-like domain walls with a two-dimensional distribution of the magnetization **M** and an almost closed magnetic flux [1, 2, 11, 12]. Similar domain walls have also been found in single-crystal films with a lattice of cubic symmetry (see [13] and references therein). It has turned out that, in this case, the surface orientation of the films with respect to the crystallographic axes exerts a significant influence on the domain wall structure. In particular, it has been shown that multi-vortex structures can arise depending on the film thickness at a specific orientation of the surface and the crystallographic axes. This result indicates that there is a need to investigate multi-dimensional structures of the magnetization in tetra-axial magnetic films. This type of anisotropy is observed in yttrium iron garnet or nickel films. Domain walls with a multi-dimensional distribution of the magnetization in films of this type have not yet been considered. However, it can be expected that, in these films, as well as in triaxial magnetic films of iron-type materials, domain wall structures may exhibit their own nontrivial features. Note that Shumate [17] estimated the contribution from the tetra-axial anisotropy to the energy of an individual twisted domain wall.

Another important problem is to investigate the process of transformation of the domain structure, which occurs with a decrease in the quality factor from a value larger than unity to a value smaller than unity. The two formulated problems can be combined by considering films that have simultaneously both the tetra-axial crystallographic and induced uniaxial perpendicular anisotropies. It should be noted that these films exist in reality (yttrium iron garnet films with rare-earth additives [18]).

As a rule, the crystallographic anisotropy in real films is small in comparison with the induced uniaxial anisotropy; however, the results presented in this paper go beyond this limitation. This is justified by the lack of reasons that could not afford to obtain films with any ratio between the induced and tetra-axial crystallographic anisotropies. The only limitation which we have used in the calculations is that the surface of the film coincides with the (111) crystallographic plane. Note that these films also exist in reality.

2. STATEMENT OF THE PROBLEM

We consider a magnetic film with linear dimensions L_x, L_y, and L_z. Let us assume that the coordinate axes x and z lie parallel to the film surface, whereas the y axis, which is directed along the normal to the film surface, coincides with the crystallographic direction [111]. In this paper, we will not consider transition magnetic structures with an essentially three-dimensional distribution of the magnetization (Bloch lines and points on the two-dimensional domain walls). Therefore, we can consider that $L_z \longrightarrow \infty$ and the magnetization **M** is a function of two coordinates:

$$\mathbf{m} = \frac{\mathbf{M}}{M_s} = \mathbf{m}(x, y) \text{ (two-dimensional model).}$$

The equilibrium distribution of the magnetization **m** can be found by minimizing the functional of the total energy of the system per unit length along the z axis. We will take into account the exchange, magnetically anisotropic, and magnetostatic interactions. Therefore, the expression for the energy functional has the following form:

$$E = \int_0^{L_x}\int_0^{L_y}(f_e + f_m + f_a)\,dx\,dy,$$

$$f_e = A\left\{\left(\frac{\partial \mathbf{m}}{\partial x}\right)^2 + \left(\frac{\partial \mathbf{m}}{\partial y}\right)^2\right\}, \quad f_m = -\frac{1}{2}M_s\mathbf{m}\mathbf{H}^{(m)},$$

$$f_a = K_u(m_x^2 + m_y^2) + K_1\left(\frac{1}{4}m_x^4 + \frac{1}{3}m_y^4 + \frac{1}{4}m_z^4\right. \tag{1}$$

$$-\frac{\sqrt{2}}{3}\sin 3\varphi m_x^3 m_y + \frac{\sqrt{2}}{3}\cos 3\varphi m_y m_z^3 + \frac{1}{2}m_x^2 m_z^2$$

$$\left. -\sqrt{2}\cos 3\varphi m_x^2 m_y m_z + \sqrt{2}\sin 3\varphi m_x m_y m_z^2\right),$$

where f_e, f_m, and f_a are the bulk energy densities of the exchange, magnetostatic, and magnetically anisotropic interactions, respectively; A is the exchange parameter; $\mathbf{H}^{(m)}$ is the magnetostatic field obtained by solving the equations of magnetostatics with the usual boundary conditions; K_u is the uniaxial anisotropy constant; K_1 is the tetra-axial anisotropy constant; and φ is the angle between the z axis and the crystallographic direction $[11\bar{2}]$ (see Fig. 1). The expression for the contribution to the energy density of the magnetically anisotropic interaction corresponding to the tetra-axial anisotropy is obtained as a result of the transition from the coordinate system related to the crystallographic axes [100], [010], and [001] (compo-

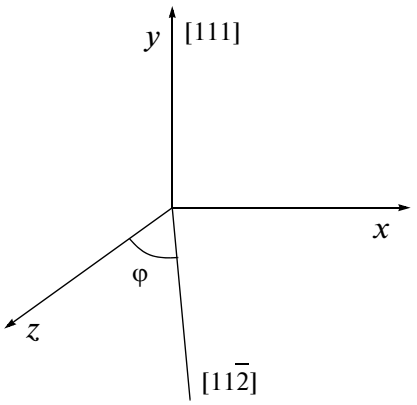

Fig. 1. Orientation of the crystallographic directions and coordinate axes.

nents with the tilde) to the coordinate system related to the film (components without the tilde):

$$\begin{aligned}\tilde{m}_x &= \frac{1}{\sqrt{3}}m_y + \frac{1}{\sqrt{6}}(m_z\cos\varphi + m_x\sin\varphi)\\ &\quad - \frac{1}{\sqrt{2}}(m_x\cos\varphi - m_z\sin\varphi),\\ \tilde{m}_y &= \frac{1}{\sqrt{3}}m_y + \frac{1}{\sqrt{6}}(m_z\cos\varphi + m_x\sin\varphi)\\ &\quad + \frac{1}{\sqrt{2}}(m_x\cos\varphi - m_z\sin\varphi),\\ \tilde{m}_x &= \frac{1}{\sqrt{3}}m_y - \sqrt{\frac{2}{3}}(m_z\cos\varphi + m_x\sin\varphi),\end{aligned} \quad (2)$$

provided that, in the coordinate system related to the crystallographic axes, the tetra-axial anisotropy energy has the standard form

$$K_1(\tilde{m}_x^2\tilde{m}_y^2 + \tilde{m}_y^2\tilde{m}_z^2 + \tilde{m}_z^2\tilde{m}_x^2), \quad K_1 < 0. \quad (3)$$

In the subsequent analysis, if not stated otherwise, we will use the coordinate system related to the film (Fig. 1) and restrict ourselves to the case $\varphi = 0$.

Under these assumptions, the numerical simulation of the domain structure of the film can be carried out using one of two approaches. The first approach is to impose periodic boundary conditions along the x axis. In this case, the period of the observed domain structure should be equal to L_x/N, $N = 1, 2, 3$ ..., so that there arises a necessity to select the dimension L_x in such a way as to reach the minimum of the energy functional (1). This method of calculation was implemented in [9, 10] for films with perpendicular magnetic anisotropy and in [16] for films with oblique anisotropy. The second approach is that the size of the film along the x axis is chosen to be finite but large enough, so that the calculated domain structure would

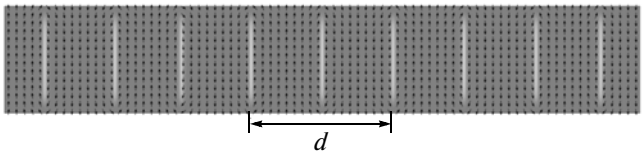

Fig. 2. Complete equilibrium distribution of the magnetization in the xy plane. The transition from white to gray color corresponds to the change from $m_z = -1$ to $m_z = 0$. $K_u = 2 \times 10^5$ erg/cm^3, $K_1 = -6500$ erg/cm^3.

have a fairly universal character. In this study, we use the second approach.

The calculations were carried out with the following parameters: $L_y = 1$ μm (film thickness), $L_x = 6$ μm (unless otherwise specified), $A = 4.15 \times 10^{-7}$ erg/cm, $M_x = 140$ G, and $K_1 = -6500$ erg/cm^3 (parameters of yttrium iron garnet). The quantity K_u was considered a variable and varied in the range from 2×10^5 erg/cm^3 to zero with a minimum step of 1000 erg/cm^3. For each nonzero value of K_u, we compared the results of calculations performed in the presence and in the absence of tetra-axial anisotropy ($K_1 = 0$). The calculations were performed with the OOMMF software package [19, 20] with discretization on a rectangular grid with a step of 5 nm in each coordinate, which did not exceed the size of the absolute single-domain state $\sim\sqrt{A/2\pi M_s^2}$.

3. RESULTS AND DISCUSSION

Figure 2 shows a distribution of the magnetization in the xy plane, which was obtained at $K_u = 2 \times 10^5$ erg/cm^3 and represents a periodic domain structure where domains with $\mathbf{m}(0, 1, 0)$ and $\mathbf{m}(0, -1, 0)$ are separated by conventional twisted domain walls. The period d of the domain structure, which corresponds to the minimum of the energy functional (1), will be hereinafter denoted as d_m. The value of d_m was determined from the calculated dependence $\gamma(d)$, where $\gamma = E/L_x$ is the total energy of the system per unit area in the xz plane (Fig. 3a). For large values of K_u, the presence of the tetra-axial anisotropy has no significant effect on the value of d_m and on the distribution of the magnetization in domains and domain walls. For $K_u = 2 \times 10^5$ erg/cm^3, we also performed calculations at $L_x = 12$ μm. For this case, we obtained the value of d_m, which differs by only 5% from the corresponding value at $L_x = 6$ μm. The dependence $d_m(K_u)$ is shown in Fig. 3b. It can be seen from this figure that, initially, with a decrease in K_u, the period d_m of the domain structure slightly decreases, which is explained by a simple lowering in the energy of the domain wall. As a result, it becomes possible to decrease the magnetostatic energy of the domain structure as a whole due to

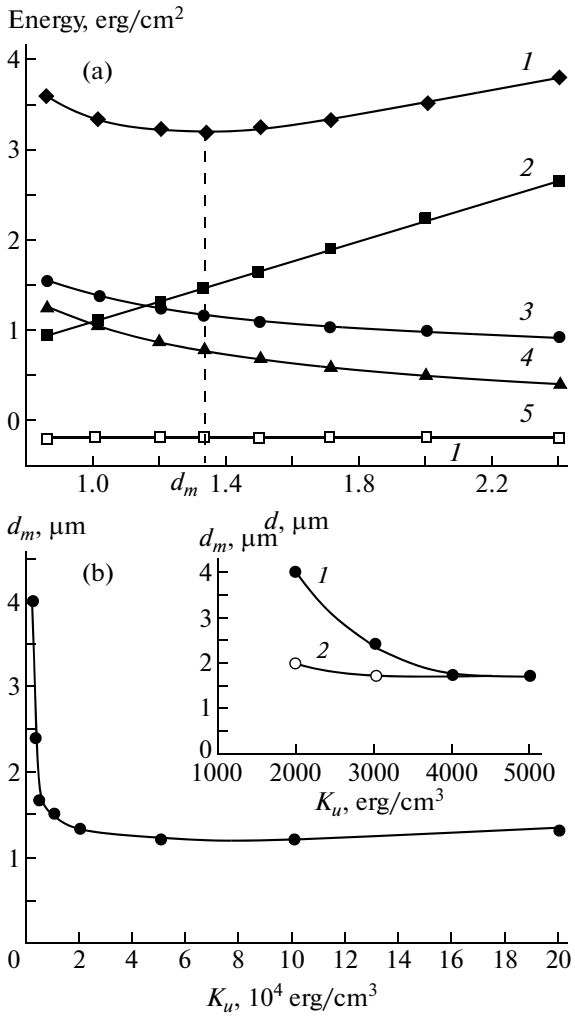

Fig. 3. (a) Dependences of the (*1*) total, (*2*) magnetostatic, (*3*) magnetically anisotropic associated with uniaxial anisotropy, (*4*) exchange, and (*5*) magnetically anisotropic associated with tetra-axial anisotropy energies of the considered system per unit area in the *xz* plane on the period of the domain structure with $K_u = 2 \times 10^5$ erg/cm^3 and $K_1 = -6500$ erg/cm^3. (b) Dependence of the period of the domain structure corresponding to the state with the minimum energy on the uniaxial anisotropy constant: (*1*) $K_1 = -6500$ erg/cm^3 and (*2*) $K_1 = 0$.

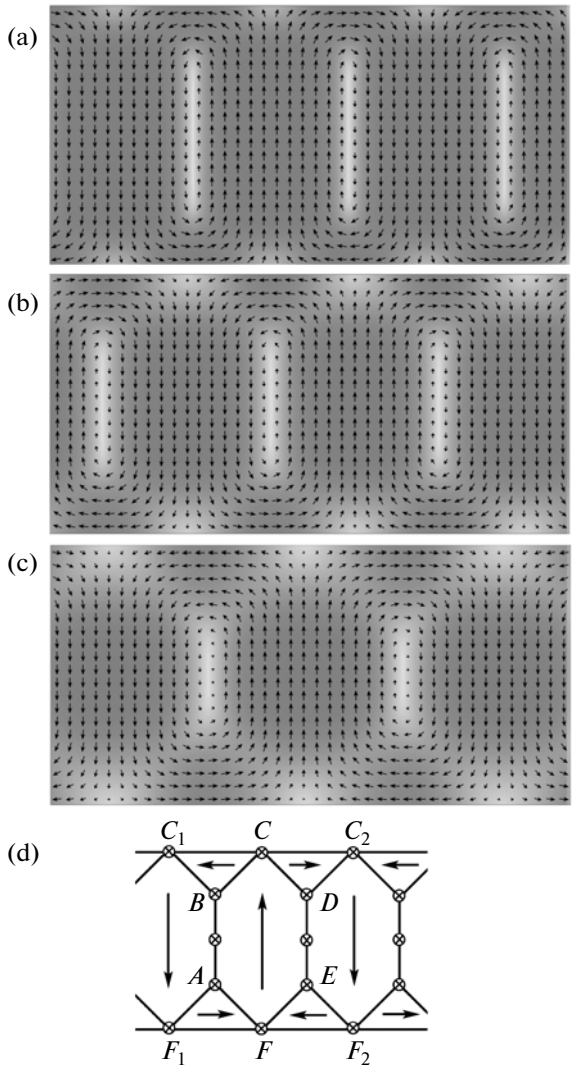

Fig. 4. (a–c) Fragments of the equilibrium distribution of the magnetization at (a) $K_u = 4 \times 10^4$ erg/cm^3, (b) $K_u = 2 \times 10^4$ erg/cm^3, and (c) $K_u = 10^4$ erg/cm^3 in the *xy* plane. The transition from white to gray color corresponds to the change from $m_z = -1$ to $m_z = 0$. (d) Schematic illustration of the equilibrium distribution of the magnetization in the *xy* plane at $K_u = 10^4$ erg/cm^3. $K_1 = -6500$ erg/cm^3.

the partition of the film into a larger number of domains. Then, however, the period d_m begins to increase rapidly due to a qualitative change in the character of the distribution of the magnetization **m** in the computational region, as will be described below.

As the uniaxial anisotropy constant K_u decreases, the magnetization in domains gradually deviates in the vicinity of the film surface from the direction *y* (far away from the surface and from the domain wall, as before, we have **m**(0, ±1, 0); see Fig. 4a), thus decreasing the density of magnetostatic poles on these surfaces and hence decreasing the magnetostatic energy. With a further decrease in the uniaxial anisotropy constant, the aforementioned regions, in which the magnetization **m** is tilted from the direction of the easy magnetization axis, grow and the tilting angle increases to the extent that the magnetization at the surface lies in the *xz* plane. At the same time, the domain wall regions expand along the *x* axis, whereas the period d_m increases. These processes result in the formation of the magnetization distribution with a magnetic flux closed in the sample. The relative magnetostatic component of the total energy of this distribution is small. This distribution of the magnetization **m** (Figs. 4b and 4c) resembles that of the Landau–Lif-

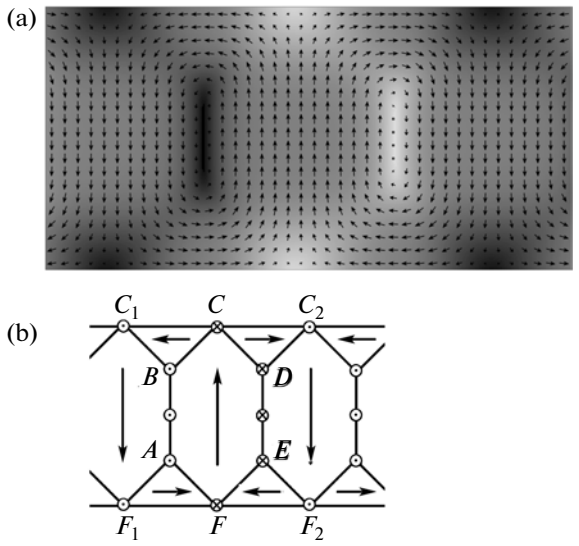

Fig. 5. (a) Fragment and (b) schematic illustration of the equilibrium distribution of the magnetization in the *xy* plane (metastable case). The transition from white to black color corresponds to the change from $m_z = -1$ to $m_z = 1$. $K_u = 10^4$ erg/cm^3, $K_1 = -6500$ erg/cm^3.

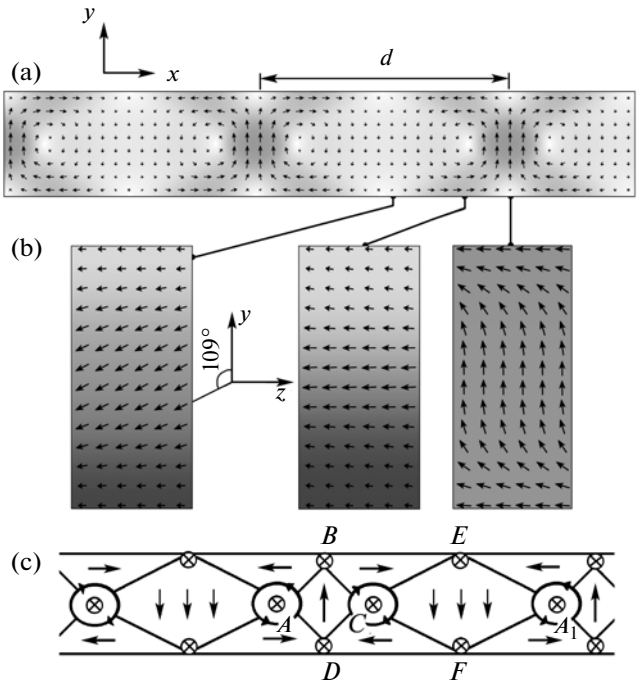

Fig. 6. (a) Complete equilibrium distribution of the magnetization in the *xy* plane. The transition from white to gray color corresponds to the change from $m_z = -1$ to $m_z = 0$. (b) Fragments of the equilibrium distribution of the magnetization in the *yz* plane. The transition from white to black color corresponds to the change from $m_x = -1$ to $m_x = 1$. (c) Schematic illustration of the equilibrium distribution of the magnetization in the *xy* plane. $K_u = 3000$ erg/cm^3, $K_1 = -6500$ erg/cm^3.

shitz structure, but with substantial differences from it. These differences are conveniently analyzed using the scheme shown in Fig. 4d. The domain wall thicknesses here cannot be considered to be small with respect to the size of domains. In the vicinity of the lines *AB* and *DE*, there are twisted domain walls with a two-dimensional structure. At the points *C*, C_1, C_2, *F*, F_1, and F_2, the direction of the magnetization **m** is collinear with the direction of the *z* axis. The lines *BC*, *CD*, *EF*, and *FA* can be considered as 90-degree domain walls. The lowest energy is observed in the structure in which the magnetization directions in all lines of the *AB* type and at points of the *C* and *F* types coincide. In this case, along all lines of the *BC* type, the magnetization **m** deviates from the *xy* plane in the same direction, thus lowering the exchange energy. In the case of the structure illustrated in Fig. 5, we have **m**(0, 0, 1) on the *AB* line and **m**(0, 0, −1) at the *C* point; as a result, the magnetization must be rotated through 180° along the *BC* line. This increases the exchange energy, so that the structure is metastable. Also a metastable structure is the structure in which all regions on the *AB*-type lines are identically magnetized (twisted domain walls have the same polarization), whereas the magnetization directions at the points *C* and *F* alternate. It is clear, however, that the circumstances may change with a decrease in the size L_z. The calculations performed for $K_1 = 0$ with constant other parameters lead to similar distributions of the magnetization. Thus, the tetra-axial magnetic anisotropy at the chosen ratio of K_1 and K_u does not play a decisive role in the formation of the structures shown in Figs. 2–5.

The magnetization distributions similar to those shown in Figs. 4b and 4c were obtained in [16], but there are significant differences: because of the easy magnetization axis tilted to the film plane [16], the magnetization **m** deviated from the direction *y* in the *ABCDEF* regions. This deviation eventually led to the fact that the directions of the magnetization **m** at the points *C* and *F* alternated.

It should be noted that, although the duration of the calculations can be significantly decreased by properly choosing more suitable initial magnetization distributions, we managed to obtain a periodic distribution of the magnetization **m** even with nonperiodic initial configurations.

The tetra-axial magnetic anisotropy significantly affects the distribution of the magnetization **m** corresponding to the minimum of the energy γ at $K_u \leq 3000$ erg/cm^3. As can be seen from Fig. 6, the character of the domain structure for $\gamma = \gamma(d_m)$ (Fig. 7a) in this case radically changes. For the analysis of the obtained structure, we again use the schematic diagram (Fig. 6c). Now, in the central part of the film, there are alternating domains with **m**(0, 1, 0) and with

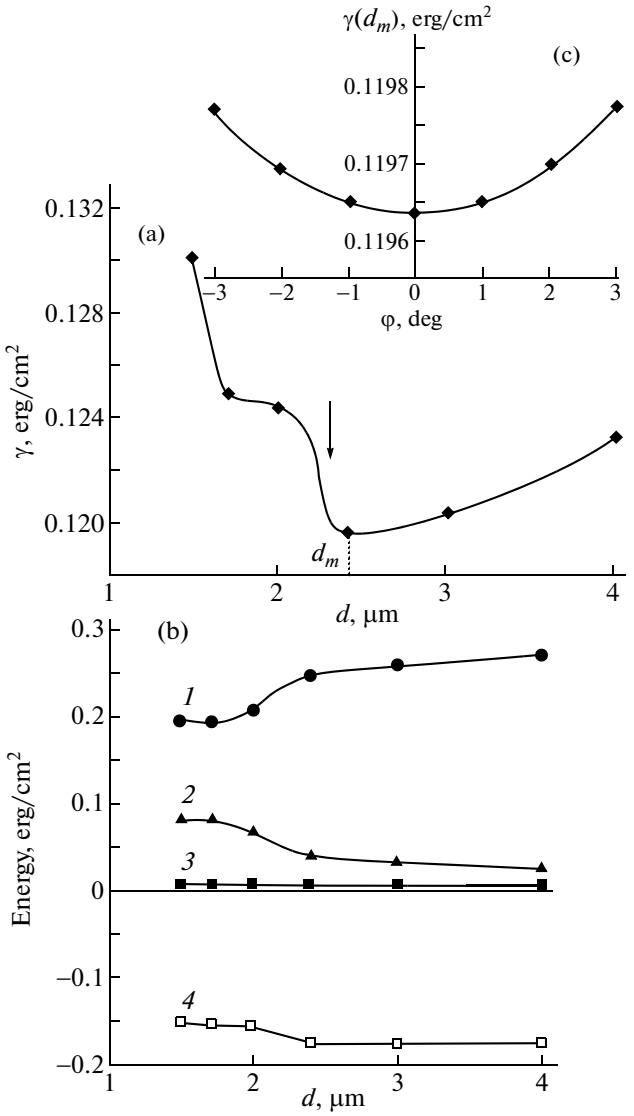

Fig. 7. (a) Dependence of the total energy $\gamma = E/L_x$ of the considered system per unit area in the xz plane on the period of the domain structure and (b) similar dependences for the (*1*) magnetically anisotropic associated with uniaxial anisotropy, (*2*) exchange, (*3*) magnetostatic, and (*4*) magnetically anisotropic associated with tetra-axial anisotropy energies constituting the energy γ. To the left of the black arrow, there are domain structures with 180-degree domain walls, and to the right of the black arrow, domain structures with 109-degree domain walls. (c) Dependence of γ on the small changes in the angle φ at $d = d_m$. $K_u = 3000$ erg/cm^3, $K_1 = -6500$ erg/cm^3.

$\mathbf{m}\left(0, -\frac{1}{3}, -\frac{2\sqrt{2}}{3}\right)$ represented in Fig. 6c by regions of the types *ABCD* and CEA_1F, respectively. The direction $\mathbf{m}\left(0, -\frac{1}{3}, -\frac{2\sqrt{2}}{3}\right)$ is parallel to one of the easy magnetization axes corresponding to the tetra-axial anisotropy at $\varphi = 0$, namely, to the crystallographic direction $[11\bar{1}]$. Closer to the surface of the film, there are regions of the types *BCE* and *DCF*, closing the magnetic flux. This distribution of the magnetization **m** significantly decreases the magnetostatic energy of the sample at a sufficiently low total magnetic anisotropy energy (Fig. 7b). As for the structures discussed above, the lowest energy is observed in the domain structure in which the directions of the magnetization at all points of the types *A*, *B*, *C*, *D*, *E*, and *F* coincide (we turn our attention once again to the fact that this result relates to $L_z \longrightarrow \infty$). The sizes of regions of the *ABCD* type are smaller than those of the CEA_1F type. At the film surface in the vicinity of the points *B*, *E*, *D*, and *F*, the magnetization is oriented opposite to the direction of the z axis. The angle between this direction and the direction of the magnetization **m** for the *ABCD* region is greater than that for the CEA_1F region; therefore, the gradient and divergence of the magnetization **m** (and, hence, the densities of the exchange and magnetostatic energies) with approaching the film surface grow more rapidly in the first of these regions. This explains their different lengths. It should be noted that Fig. 6c is only a simplified diagram, which facilitates perception. Actually, the magnetization **m** in the domain structure shown in Fig. 6a varies smoothly, so that the magnetization has exactly the directions $\mathbf{m}(0, 1, 0)$ and $\mathbf{m}\left(0, -\frac{1}{3}, -\frac{2\sqrt{2}}{3}\right)$ only in the central part of the regions *ABCD* and CEA_1F.

It has been found that the domain structure illustrated in Fig. 6 is stable with respect to small changes in the angle φ in the vicinity of zero; in this case, the local minimum of the energy γ corresponds to $\varphi = 0$ (Fig. 7c). For 3000 erg/cm^3 < K_u < 6000 erg/cm^3 and $K_1 = -6500$ erg/cm^3, this domain structure existed as a metastable structure (the stable structure was similar to that shown in Fig. 4c), and with a further increase in K_u, it became unstable.

The regions *ABCD* and CEA_1F are separated by domain walls of a completely new type, namely, by 109-degree vortex-like walls (Fig. 6b). These domain walls exhibit a feature that distinguishes them from the conventional twisted domain walls (Fig. 4) and from the 180-degree vortex-like domain walls, which are characteristic of the geometry with the easy magnetization axis lying in the film plane (see, for example, [1, 2, 11, 12]). This feature lies in the fact that the polarization of a 109 degree vortex-like domain wall (taken as ±1 for two possible directions of the magnetization $\mathbf{m}(0, 0, \pm 1)$ at the points *A*, *C*, and A_1 in Fig. 6c) cannot take on values in an arbitrary way and is determined by the orientation of the magnetization **m** in the neighboring domains. In the case illustrated in Fig. 6, at the points *A*, *C*, and A_1, the magnetization can be directed only against the direction of the z axis. A similar domain wall with opposite polarization (in the afore-

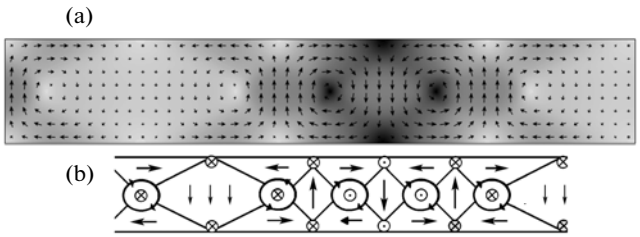

Fig. 8. (a) Complete equilibrium distribution of the magnetization and (b) schematic illustration of this distribution in the *xy* plane (metastable case). The transition from white to black color corresponds to the change from $m_z = -1$ to $m_z = 1$. $K_u = 3000$ erg/cm^3, $K_1 = -6500$ erg/cm^3.

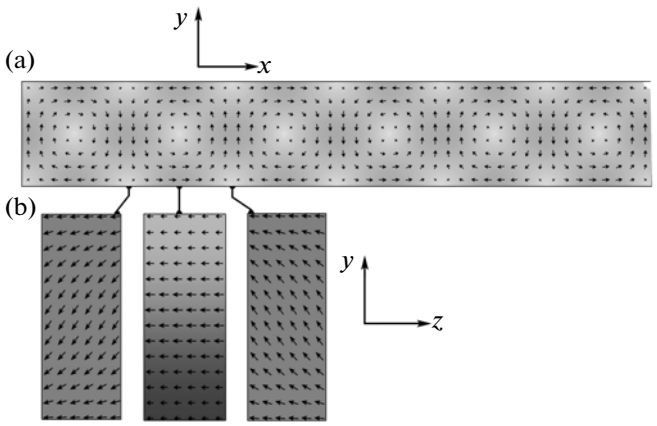

Fig. 9. (a) Complete equilibrium distribution of the magnetization in the *xy* plane. The transition from white to gray color corresponds to the change from $m_z = -1$ to $m_z = 0$. (b) Fragments of the equilibrium distribution of the magnetization in the *yz* plane. The transition from white to black color corresponds to the change from $m_x = -1$ to $m_x = 1$. $K_u = 2000$ erg/cm^3, $K_1 = 0$.

mentioned points, the magnetization **m** has the direction of the *z* axis) at $\varphi = 0$ will separate domains with $\mathbf{m}(0, -1, 0)$ and $\mathbf{m}\left(0, \frac{1}{3}, \frac{2\sqrt{2}}{3}\right)$. The domain structure with such domains is energetically equivalent to that shown in Fig. 6. There can also exist intermediate metastable variants. An example of one of these variants is shown in Fig. 8.

For $K_u = 3000$ erg/cm^3, the described results were also reproduced at $L_x = 12$ μm (i.e., in this case, too, we obtain domain structures with walls of the same type and with the same value of d_m). The question about the influence of the magnetostriction on the stability of 109-degree domain walls remains open. It is possible, however, that, in the considered situation there is an analogy with the case of cubic crystals, when within a one-dimensional model of the distribution of the magnetization **m**, the magnetostriction plays a decisive role in the formation of domain walls (preventing the decomposition of a 180-degree wall into two 90-degree walls), but it does not play the same role upon the transition to a two-dimensional model.

For $K_1 = 0$, the structures similar to those shown in Figs. 6 and 8 are unstable. Instead, in the range from $K_u = 10^4$ erg/cm^3 to $K_u = 2000$ erg/cm^3, there is a domain structure similar to that shown in Fig. 4c. With a decrease in the uniaxial anisotropy constant, this domain structure undergoes the following changes: the period d_m slightly increases (Fig. 3b), the relative sizes of regions of the types BC_1C and AFF_1 increase (Fig. 4d), the domain walls extend along the *x* axis, and the magnetization in regions of the *ABCDEF* type gradually begins to deviate from the direction of the easy magnetization axis (the *y* axis). The described changes, which entail the decrease in the magnetostatic and exchange energies with increasing weakening of the influence of the magnetically anisotropic interaction, at $K_u = 2000$ erg/cm^3 lead to the formation of the structure shown in Fig. 9. In this case, over the entire computational region, the magnetization **m** deviates from the *xy* plane, thus forming an obtuse (or acute) angle with the *z* axis, and nowhere is directed along the easy magnetization axis. As can be seen, the domains and domain walls in this structure have very close sizes, so that the mental separation of these elements becomes difficult.

For $K_u = 1000$ erg/cm^3 and $K_1 = 0$, the lowest energy is observed in the state with a uniform magnetization along the *z* axis. This result is consistent with the analytical formula for the thickness of nucleation of stripe domains in a zero field $D_c = 2\pi\sqrt{\frac{A}{K_u}}$ [21], which for a given value of the uniaxial anisotropy constant gives the value of 1.28 μm. This state is also stable at $K_u \le 1000$ erg/cm^3 in the presence of the tetra-axial anisotropy. Although the *y* axis is directed parallel to the common easy magnetization axis for both types of anisotropy, another easy magnetization axis (crystallographic direction $[11\bar{1}]$) is oriented close enough to the *z* axis. As a result, the distribution with a uniform orientation of the magnetization $\mathbf{m}(0, 0, \pm 1)$ has a sufficiently low energy of the tetra-axial magnetic anisotropy. Together with the zero exchange and magnetostatic energies (at $L_z \longrightarrow \infty$), this makes such a distribution energetically favorable at sufficiently low values of K_u. In this case, as the transition state there arises a domain structure in which regions of the CEA_1F types (Fig. 6c) grow in length along the *x* axis, and the magnetization **m** in their central part lies in the direction opposite to the *z* axis (Fig. 10). The 109-degree vortex-like domain walls transform into 90-degree vortex-like walls. The causes for the formation of this domain structure are clear, when taking into account all the above considerations.

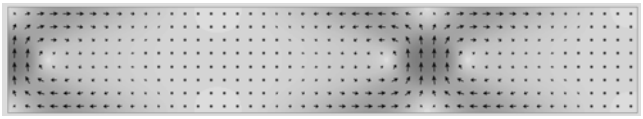

Fig. 10. Complete equilibrium distribution of the magnetization in the *xy* plane. The transition from white to gray color corresponds to the change from $m_z = -1$ to $m_z = 0$. $K_u = 2000$ erg/cm^3, $K_1 = -6500$ erg/cm^3.

It is interesting that, at $K_u \le 1000$ erg/cm^3, on a certain set of initial distributions of the magnetization, we obtained a structure consisting of domains with alternating directions of the magnetization $\mathbf{m}(0, 0, \pm 1)$, separated by a vortex-like Bloch domain walls [1, 2, 11, 12]. This domain structure was always metastable, which, however, can be not the case for finite values of L_z.

4. CONCLUSIONS

The dependence of the character of the domain structure of thin films with perpendicular magnetic anisotropy on the uniaxial anisotropy constant K_u over a wide range of values in the presence (absence) of tetra-axial magnetic anisotropy has been investigated using the numerical micromagnetic simulation within a two-dimensional model of the magnetization distribution with the exact (model-free) consideration of the main interactions, including the magnetostatic one.

(1) It has been found that, with a decrease in the uniaxial anisotropy constant K_u, the domain structure with domains magnetized along the normal to the film surface transforms into the domain structure with a closed magnetic flux, which resembles the Landau–Lifshitz structure, but with substantial differences from it.

(2) The transition between the aforementioned types of domain structures has been investigated in detail for the first time. It has been demonstrated that, with a decrease in K_u, the Néel sections of twisted walls in films with $Q > 1$ gradually expand into the domain region, thus eliminating the magnetostatic poles in the open domain structure.

(3) It has been shown that the transition to the state with a magnetic flux almost closed inside the film depends on the ratio of the induced and natural crystallographic anisotropy constants. The range of variation in the values of K_u has been found, where the formed domain structures are similar to each other both in the presence and in the absence of tetra-axial magnetic anisotropy.

(4) New types of micromagnetic magnetization configurations have been predicted, such as 109-degree and 90-degree vortex-like domain walls and periodic domain structures, including these domain walls and domains of different widths. The physical causes for the formation of a new type of micromagnetic structures have been determined.

ACKNOWLEDGMENTS

This study was supported by the Russian Foundation for Basic Research (project no. 11-02-00931) and the Department of the Physical Sciences of the Russian Academy of Sciences (program no. 12-T-2-1007).

REFERENCES

1. A. E. La Bonte, J. Appl. Phys. **40**, 2450 (1969).
2. B. N. Filippov and L. G. Korzunin, Fiz. Met. Metalloved. **75**, 49 (1993).
3. C. C. Shir and J. S. Lin, J. Appl. Phys. **50**, 2270 (1979).
4. N. Hayashi, Y. Nakatani, and T. Inoue, Jpn. J. Appl. Phys. **27**, 366 (1988).
5. K. Ramstöck, T. Leibl, and A. Hubert, J. Magn. Magn. Matter. **135**, 97 (1994).
6. C. J. Garcia-Cervera, Bol. Soc. Esp. Mater. Appl. **39**, 103 (2007).
7. L. I. Antonov, S. G. Osipov, and M. M. Khapaev, Fiz. Met. Metalloved. **55**, 917 (1983).
8. L. I. Antonov, S. G. Osipov, and M. M. Khapaev, Fiz. Met. Metalloved. **57**, 892 (1984).
9. L. I. Antonov, V. V. Ternovskii, and M. M. Khapaev, Fiz. Met. Metalloved. **67**, 53 (1989).
10. L. I. Antonov, S. V. Zhuravlev, E. V. Lukasheva, and A. N. Matveev, Fiz. Met. Metalloved. **67**, 23 (1992).
11. B. N. Filippov, Low Temp. Phys. **28** (10), 707 (2002).
12. K. Ramstöck, W. Hartung, and A. Hubert, Phys. Status Solidi A **155**, 505 (1996).
13. B. N. Filippov and F. A. Kassan-Ogly, Phys. Met. Metallogr. **110**, 642 (2010).
14. L. D. Landau and E.M. Lifshitz, Phys. Z. Sowjetunion **8**, 155 (1935).
15. E. Schlomann, J. Appl. Phys. **44**, 1837 (1973).
16. M. La Brune and J. Miltat, J. Appl. Phys. **75**, 2156 (1994).
17. P. W. Shumate, J. Appl. Phys. **44**, 5075 (1973).
18. F. V. Lisovskii, *Physics of Cylindrical Magnetic Domains* (Sovetskoe Radio, Moscow, 1978) [in Russian].
19. M. J. Donahue and D. G. Porter, *OOMMF User's Guide: Version 1.0, NISTIR 6376* (National Institute of Standards and Technology, Gaithersburg, Maryland, 1999).
20. K. M. Lebecki, M. J. Donahue, and M. W. Gutowski, J. Phys. D: Appl. Phys. **41**, 175005 (2008).
21. A. Hubert, IEEE Trans. Magn. **21**, 1604 (1985).

Translated by O. Borovik-Romanova